International Journal of Automotive Technology, Vol. 7, No. 3, pp. 289–294 (2006)

1229-9138/2006/027-08

IN-CYLINDER FLOW ANALYSIS USING WAVELET ANALYSIS

D. PARK*, P. E. SULLIVAN and J. S. WALLACE

University of Toronto, Toronto, ON, M5S 3G8, Canada

(Received October 25, 2005; Revised December 23, 2005)

Abstract–Better fundamental understanding of the interactions between the in-cylinder flows and combustion process is an important requirement for further improvement in the fuel economy and emissions of internal combustion (IC) engines. Flow near a spark plug at the time of ignition plays an important role for early flame kernel development (EFKD). Velocity data measurements in this study were made with a two-component laser Doppler velocimetry (LDV) near a spark plug in a single cylinder optical spark ignition (SI) engine with a heart-shaped combustion chamber. LDV velocity data were collected on an individual cycle basis under wide-open motored conditions with an engine speed of 1,000 rpm. This study examines and compares the flow fields as interpreted through ensemble, cyclic and discrete wavelet transformation (DWT) analysis. The energy distributions in the non-stationary engine flows are also investigated over crank angle phase and frequency through continuous wavelet transformation (CWT) for a position near a spark plug. Wavelet analysis is appropriate for analyzing the flow fields in engines because it gives information about the transient events in a time and frequency plane. The results of CWT analysis are provided and compared with the mean flows of DWT first decomposition level for all cycles at a position. Low frequency high energy found with CWT corresponds well with the peak locations of the mean velocity. The high frequency flows caused by the intake jet gradually decay as the piston approaches the bottom dead center (BDC).

KEY WORDS : Internal combustion (IC), Early flame kernel development (EFKD), Laser Doppler velocimetry (LDV), Discrete wavelet transformation (DWT), Discrete wavelet transformation (DWT), Bottom dead center (BDC)

1. INTRODUCTION

In recent years, efforts have focused on improving fuel economy and exhaust emissions by changing the combustion chamber and intake system geometries in IC engines. Better understanding of in-cylinder flow processes on combustion will allow improved fuel economy and emissions of IC engines. Although in-cylinder velocities have been studied for many years, decomposition into mean and turbulence velocities remains subjective. It is difficult to decompose velocity fields in IC engines as the flow field is non-stationary and highly three-dimensional (Catania and Mittica, 1989). In determining the mean and turbulence velocity for engine flows, ensemble and cyclic averages have been used. The ensemble averaged mean velocity is calculated by binning instantaneous cycle velocities over a crank angle degree range and averaging over individual cycles.

Ensemble averaging limitations include: (i) the turbulence energy obtained from ensemble averaging is overestimated by including the quasi-periodic bulk flows (Liou and Santavicca, 1985) and (ii) there are no cyclic variations of the mean velocity between cycles. Cyclic averaging uses a low-pass filtering to overcome this problem. Cyclic averages have still difficult as (i) the filtering frequencies are well defined either in temporal or frequency space, but not both and (ii) the turbulence velocity found depends on the cut-off frequency selected. Wavelet transformation decomposes the flow based on energy distributions with compact functions defined in both spaces at the same time.

The objective of this study is to determine the merits of wavelet analysis with respect to traditional averages, ensemble and cyclic averages. Towards this goal, velocity data were collected in a V6 3.1L optical engine under motored conditions through a two-component LDV.

Novel data processing techniques were applied to the in-cylinder velocity data. CWT is introduced to overcome the limitations of the traditional velocity reduction methods by representing both time and scale information in a plane.

2. EXPERIMENTAL SYSTEM

The experimental equipment used in this investigation is a single cylinder optical engine with a DC dynamometer

*Corresponding author. e-mail: dkpark@mie.utoronto.ca

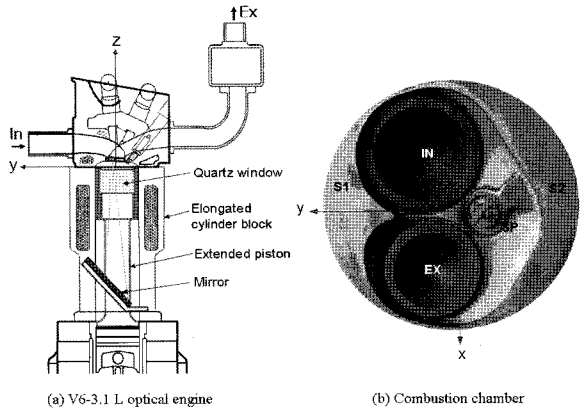

(a) V6-3.1 L optical engine (b) Combustion chamber

Figure 1. Schematics of test engine and combustion chamber.

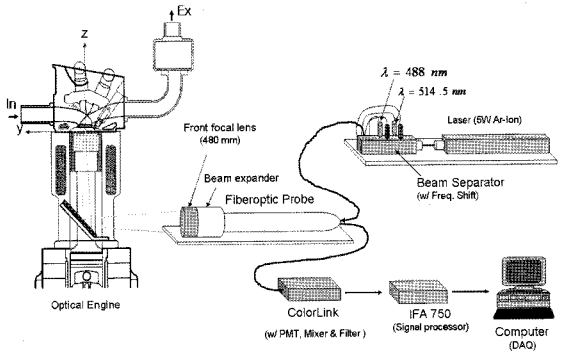

Figure 2. Schematic of LDV system.

and a two-component LDV to measure in-cylinder velocity data near the spark plug and is described below.

2.1. Test Engine

Measurements have been made in a V6 3.1 L single optical cylinder engine (Figure 1(a)). Optical access is through a flat quartz window installed at the top of an extended piston, and a mirror is mounted on an elongated cylinder block. The mirror redirects the laser beams and positions the LDV measurement volume. Three carbon piston rings with Teflon allow the engine to be operated without lubrication. A shaft encoder with a resolution of five pulses per a crank angle degree has been installed on the end of the crankshaft as a reference while collecting data. A top dead center (TDC) pulse is used for triggering and crank degree mark (CDM) pulses are used as external trigger and clock signals.

The engine used in this study has a heart shape combustion chamber with two valves (one for intake and the other for exhaust) and two squish areas (S1 and S2). Figure 1(b) shows the schematic of the bottom view of the combustion chamber.

2.2. Velocity Measurement System

2.2.1. LDV system

A two-component LDV system was used to measure the velocity data in a cylinder flow near the spark plug in this study. In-cylinder velocity data were collected under motored, wide open throttle (WOT) and 1000 rpm of the engine speed. LDV data were acquired with a maximum input rate of 20 MHz by a National Instruments DIO PCI 6534 board and the data were analyzed with software developed in-house. A schematic of the LDV system used in this study is shown in Figure 2.

The main components of the LDV are: (i) a 5W Ar-Ion laser, TSI Innova 70; (ii) a ColorBurst multi-beam separator, TSI model 9201; (iii) Fiber optic couplers, TSI model 9271; and (iv) a two-component Fiber optic probe, TSI model 9800.

2.2.2. Particle seeding system

A particle seeding system, TSI model 3400, was used to introduce particles. Kronos 2200, 0.2 mm median particle diameter TiO_2, was used as seed particles. A desiccant, Degussa R972, was added to the Kronos 2200 to prevent agglomeration of the fines and to decrease the bulk density of the mixture.

3. LDV DATA ANALYSIS

The decomposition techniques, ensemble, cyclic and wavelet averages (DWT and CWT), are described in detail and compared in the following subsections.

3.1. Ensemble Analysis

The ensemble averaged mean velocity is calculated by binning instantaneous cycle velocities over a crank angle degree range and averaging over individual cycles.

3.2. Cyclic Analysis

Cyclic averaging separates an instantaneous velocity into a non-stationary mean and a turbulence fluctuation by a low pass filtering using an inverse fast Fourier transformation (IFFT) in this study. The individual cyclic mean is the low frequency portion of the instantaneous velocity, and the high frequency portion is the turbulence. It is important to minimize arbitrariness in the choice of the cutoff frequency, yet there is no obvious criterion for selecting the cutoff frequency. The ensemble average of the individual cycle mean velocity should be the same as the conventional ensemble mean velocity (Catania and Mittica, 1989; Fansler and French, 1988):

$$\overline{\tilde{U}(k,\theta)} = \overline{U(\theta)} \tag{1}$$

The cutoff frequency used in this paper is based on the frequency of the first level DWT decomposition describ-

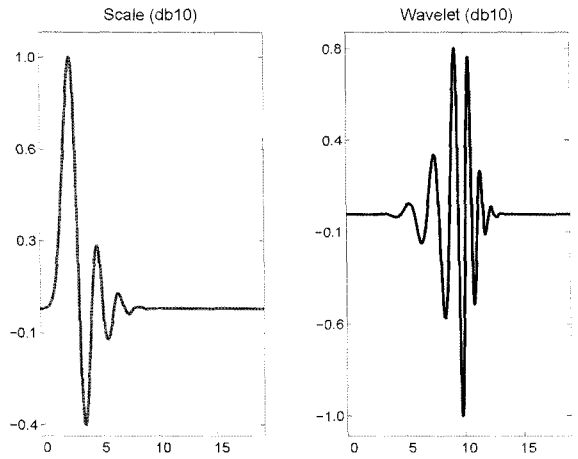

Figure 3. Wavelet scale and basis function (db10).

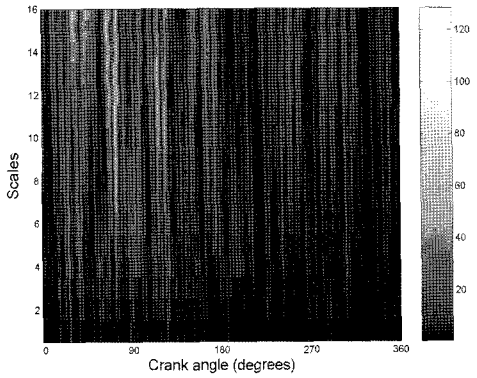

Figure 4. Schematic of CWT energy.

ed at next section as this cutoff frequency satisfies within 2% the condition of Equation 1.

The low-pass filtering frequency for this study is 1170 Hz, which is an absolute number that changes with engine speed and corresponds to 140 (engine cycle)$^{-1}$ that indicates the data of 5.1 crank angle degrees (CAD) width at the engine speed of 1000 rpm. The filtering frequency in terms of (engine cycle)$^{-1}$ represents the number of bins into which the data from an individual cycle is grouped.

3.3. Wavelet Analysis

Fourier analysis has been used to analyze the signal over the last several decades. But most interesting signals have numerous non-stationary characteristics. Therefore, different signal analysis methods have been required to interpret non-stationary signals because the Fourier transformation can not describe when a particular event took place due to the loss of time information by transforming time to frequency. Wavelet analysis localizes the signals within variable-sized regions in a time-frequency plane. Transient flow fields can be localized through the local coefficients of wavelet transformation. Wavelet analysis allows users to use the long time intervals where more precise low-frequency information is required, and shorter regions where high-frequency information is needed.

Unlike sinusoidal signals, wavelets tend to be irregular, asymmetric and localized waves and have finite duration with zero average (see Figure 3) and they are suitable for unsteady signal analysis. Fourier transformation decomposes a signal into sinusoids of various frequencies. Wavelet transformation decomposes a signal into shifted and scaled baby wavelets of a mother (original) wavelet. Wavelet transformation has been successfully applied to IC engines (Ancimer *et al.*, 2001). Two wavelets are introduced: One is the continuous wavelet transformation (CWT) and the other is the discrete wavelet transformation (DWT).

3.3.1. CWT analysis

CWT is used to decompose a velocity field u(t) using a known wavelet function $\varphi(t)$ in this study. CWT is defined as:

$$C_I(a,b)=\int_{-\infty}^{\infty} u(t)\overline{\varphi_{a,b}(t)}dt \tag{2}$$

where $\varphi_{a,b}(t)\frac{1}{\sqrt{a}}\varphi\left(\frac{t-b}{a}\right),\ a>0$

where $\overline{\varphi_{a,b}(t)}$ is a complex conjugate of $\varphi_{a,b}(t)$.

Variables a and b are called scale (dilation or compression) parameter and translation (shifting) parameter, respectively. The scale parameter a corresponds to frequency information, and the translation parameter b indicates the location of the wavelet along the time axis. $C_I(a,b)$ is a wavelet coefficient, which is a function of scale and position. $|C_I(a,b)|$ represents the CWT energy (see Figure 4).

3.3.2. DWT analysis

To improve computational speed, it is possible to use a similar approach as done with FFT's. The scales are chosen as powers of 2 and the equations become:

$$C_I(2^{-j},k2^{-j})=2^{j/2}\int_{-\infty}^{\infty} u(t)\varphi(2^j t-k)dt \tag{3}$$

and $\varphi_{j,k}=2^{j/2}\varphi(2^j t-k)$

where j and k are integers. Starting from u, the first step produces two sets of coefficients: approximation coefficient cA1, and detail coefficient cD1. These vectors are obtained by convolving u with the low-pass filter to get the approximation coefficients, and with the high-pass filter for detail coefficients.

For a sample rate f_s, and length $N=2^J$ a discrete signal u(n), is:

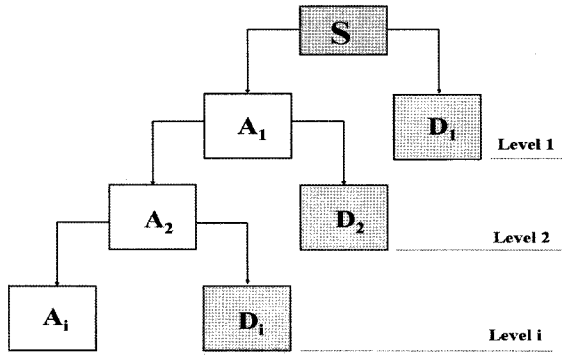

Figure 5. Wavelet decomposition, where S is a raw signal, and A_i and D_i are an approximation and a detail at a level i, respectively.

$$\begin{aligned} u(n) &= \sum_k cA_0(k)\phi_{J,k}(n) \\ &= \sum_k cA_1(k)\phi_{J-1,k}(n) + \sum_k cD_1(k)\phi_{J-1,k}(n) \\ &= \cdots\cdots \\ &= A_J(n) + \sum_{j \le J} D_j(n) \end{aligned} \tag{4}$$

where the coefficients $cA_1(k)$ and $cD_1(k)$ are the discrete wavelet coefficients of u(n), $\varphi_{J-1,k}(n)$ and $\varphi_{J-1,k}(n)$ are the orthogonal wavelet basis functions, and the wavelet scale functions, respectively. DWT maps the signal u(n) onto a two-dimensional time-frequency plane, where the scale is related to the parameter j and the position in time domain is illustrated by the translation parameter k. The signal can be further decomposed with successive approximations being decomposed in turn. The wavelet decomposition is schematically presented in Figure 5. For flow fields, the approximation A_1 is treated as the mean of the signal, the detail D_1 is the turbulence fluctuation of the first decomposition level. For decomposition level i, the mean velocity of the velocity signal is A_i, and the turbulence intensity is determined by the root mean square (RMS) of the summation of the details from the level 1 to the level i.

4. RESULTS AND DISCUSSION

The in-cylinder velocity data in the vicinity of the spark plug were collected at position A (x, y, z = 6.0 mm, –7.5 mm, 3.0 mm) near the electrode for 308 cycles under motored conditions (Figure 6).

4.1. Cyclic Analysis

A lower cutoff frequency diminishes the amplitude of the individual cycle mean velocity (Figure 7(a)). The cyclic average is limited because the turbulence energy depends on how the cutoff frequency is selected (Figure 7(b)).

The turbulence intensity is gradually increases as the cutoff frequency is decreases.

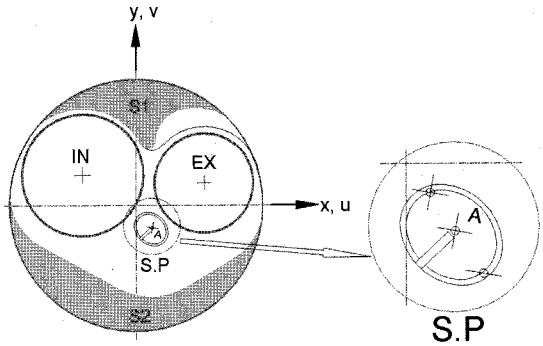

Figure 6. Measurement positions of the in-cylinder velocities (top view of combustion chamber configuration), where A is a measurement position, S1 and S2 are the squish areas, and IN and EX are the intake valve and the exhaust valve.

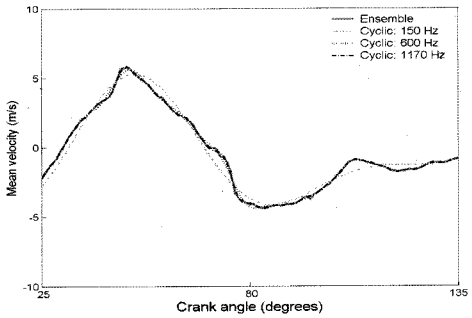

(a) Mean velocities for different cutoff frequencies

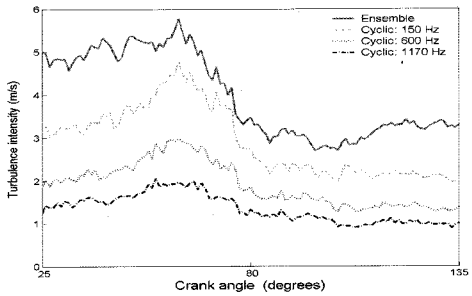

(b) Turbulence intensities for different cutoff frequencies

Figure 7. The turbulence intensities and mean velocities based on cyclic average for different frequencies, 150 Hz, 600 Hz and 1170 Hz and ensemble average.

4.2. DWT Analysis

The ensemble mean velocities for various DWT decomposition levels are shown in Figure 8(a). As the decomposition level is gradually increases, the mean velocity is smoothes, i.e. lowering the low-pass frequency of the

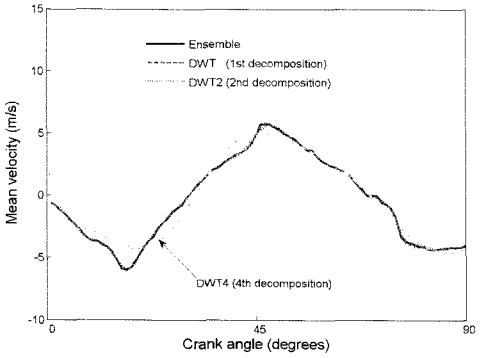

(a) Mean velocities for different DWT decomposition levels with ensemble velocity

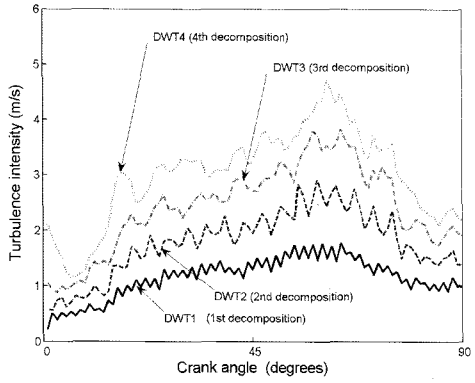

(b) Turbulence intensities for different DWT decomposition levels

Figure 8. Mean velocities and turbulence intensities of all cycles for different DWT decomposition levels at position A.

averaging. Based on this, it is suggested the DWT mean velocity should be chosen from the first level decomposition since the mean velocity of the DWT first level decomposition satisfies (within 2% error) Equation 1, as suggested by Catania and Mittica (1989). The turbulence intensity gradually increases as the DWT decomposition level is increases (see Figure 8(b)).

4.3. Flows with Respect to Different Averages

The mean and turbulence flows are characterized using ensemble, cyclic and DWT averaging techniques. Figures 9 and 10 show how different data analysis techniques influence the interpretation of mean and turbulence velocities.

4.3.1. Ensemble mean velocity

The ensemble mean velocities are almost same for the different data reduction methods, ensemble, cyclic (cutoff frequency = 1170 Hz) and DWT 1st level decomposition (Figure 9). This satisfies the requirement that the ensemble average of the individual cycle mean should be

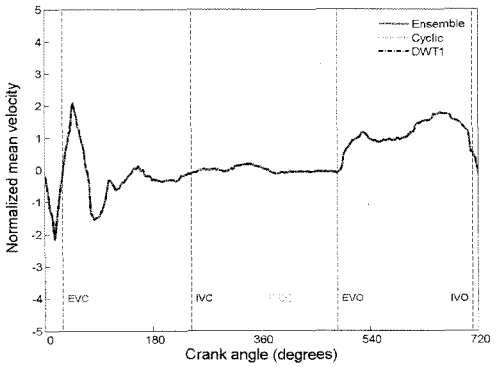

Figure 9. Ensemble mean velocities normalized by the mean piston speed (2.8 m/s at 1000 rpm) for different data reduction techniques, which are ensemble, cyclic (cutoff: 1170 Hz) and DWT first level decomposition at position A.

the same as the conventional ensemble mean velocity (Equation 1).

The statistical uncertainty for the mean velocity was evaluated with a confidence level of 95%. The standard error range of the raw and the mean velocity with cyclic averaging is 7–8%.

4.3.2. Turbulence intensity

Comparing normalized turbulence intensities, turbulence intensity/mean piston speed, calculated from cyclic averaging with a cutoff frequency of 1170 Hz and DWT first level decomposition, the turbulence intensities display similar trends and amplitudes (Figure 10).

The turbulence intensity calculated with ensemble averaging, however, has a different trend and amplitude from the other two reduction methods, cyclic and DWT. The turbulence intensity from ensemble averaging at the time of ignition is as around 2.5 times as the turbulence

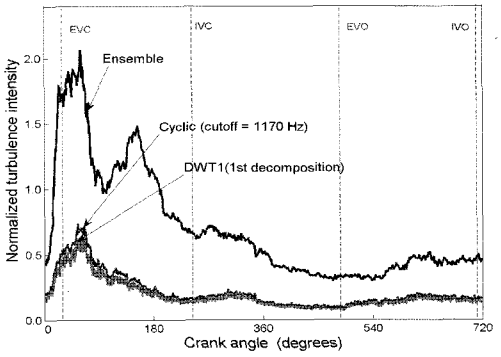

Figure 10. Turbulence intensities normalized by mean piston speed at 1000 rpm (2.8 m/s) for different reduction techniques, which are ensemble, cyclic (cutoff: 1170 Hz) and DWT first level at position A.

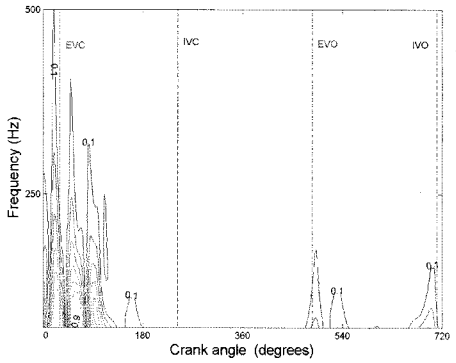

Figure 11. Ensemble averaged CWT energy normalized by maximum energy for all cycles at A (where numbers in the contours represent the normalized energy, whose high values represent high energy).

intensities of the other two reduction methods.

The statistical uncertainty for the mean velocity was evaluated with a confidence level of 95%. The standard error range of the turbulence fluctuation velocity with cyclic averaging is about 2%.

4.4. CWT Analysis

Flow energy was simultaneously visualized with the CWT over time and frequency. To interpret the energy in a time-frequency plane, the ensemble averaged CWT energy, normalized by maximum energy, for all cycles at position A was plotted in Figure 11. Figure 11 shows ensemble averaged CWT energy for all cycles at position A. The peaks of the ensemble mean velocity in Figure 9 are at 24, 46 and 83 CAD, and the peak CWT energy in Figure 11 occurs at the same locations.

The highest mean CWT energy occurs at the time when the ensemble averaged mean velocity is maximum. Large energy during intake occurs in low frequency regions (less than 200 Hz), but the energy during the compression, expansion and exhaust processes is low. There is energy with high frequencies during intake caused by turbulence production by the increased velocity gradient in the shear layer of intake jet, and then the energy gradually weakens by decreasing angular momentum as the piston approaches BDC and the piston mean speed decreases.

5. CONCLUSIONS

The conclusions of this study are summarized as follows:

(1) The velocity energy distributions are represented by CWT average contour plots with respect to a variety of scales and crank angle degrees in a time-frequency plane. The large scale high energy regions found with CWT correspond well with the peak locations of the mean velocity.

(2) There is energy with high frequencies during intake from turbulence production with high frequency by the increased velocity gradient in the shear layer of the intake jet. The high frequency energy, however, gradually decreases due to the decreasing angular momentum of swirl flow as the piston approaches BDC and the piston mean speed decreases.

(3) Though the arbitrariness associated with the decision of a cutoff frequency still exists, the frequency of the first level discrete wavelet transformation, DWT, can be used as a cutoff frequency for the filtering, because it satisfies within 2% relative error of the requirement that the ensemble average of the individual cycle mean should be the same as the conventional ensemble-mean velocity.

REFERENCES

Ancimer, R., Sullivan, P. and Wallace, J. (2001). Decomposition of measured velocity fields in spark ignition engines using discrete wavelet transforms. *Experiments in Fluids,* **30,** 237–238.

Catania, A. E. and Mittica, A. (1989). Extraction techniques and analysis of turbulence quantities from in-cylinder velocity data. *ASME J. Engineering for Gas Turbines and Power,* **111**, 466–478.

Catania, A. E. and Mittica, A. (1990). Autocorrelation and autospectra estimation of reciprocating engine turbulence. *ASME J. Engineering for Gas Turbines and Power,* **112,** 357–368.

Fansler, T. D. and French, D. F. (1988). Cycle-resolved laser-velocimetry measurements in a reentrant-bowl-in-piston engine. *SAE Paper No.* 880377.

Liou, T. M. and Santavicca, D. A. (1985). Cycle resolved LDV measurements in a motored IC engine. *ASME J. Fluids Engineering,* **107,** 232–240.

Park, D. (2005). *The Influence of Different in-Cylinder Flows on Combustion in an IC Engine.* Ph. D. Dissertation. University of Toronto.